Incorporation of Structural Tensor and Driving Force Into Log-Demons for Large-Deformation Image Registration

Ying Wen, Le Zhang, LiangHua He, and MengChu Zhou, *Fellow, IEEE*

***Abstract*— Large-deformation image registration is important in theory and application in computer vision, but is a difficult task for non-rigid registration methods. In this paper, we propose a structural Tensor and Driving force-based Log-Demons algorithm for it, named TDLog-Demons for short. The structural tensor of an image is proposed to obtain a highly accurate deformation field. The driving force is proposed to solve the registration issue of large-deformation that often causes Log-Demons to trap into local minima. It is defined as a point correspondence obtained via multisupport-region-order-based gradient histogram descriptor matching on image's boundary points. It is integrated into an exponentially decreasing form with the velocity field of Log-Demons to move the points accurately and to speed up a registration process. Consequently, the driving force-based Log-Demons can well deal with large-deformation image registration. Extensive experiments demonstrate that the TDLog-Demons not only captures large deformations at a high accuracy but also yields a smooth deformation.**

***Index Terms*— Image registration, tensor, driving force, Log-Demons algorithm, optimization.**

I. Introduction

Non-rigid image registration is a fundamental task in image processing used to match two or more pictures. It has been widely used for target recognition, remote sensing, navigation and medical diagnosis. When dealing with large-deformation image registration, it faces many challenges and has thus received much attention from many researchers [1]–[7].

The Demons algorithm is a predominant way for image registration, as proposed in Thirion's work [8]. Gradient information is important to the original Demons algorithm, which may fail to registration if such information is insufficient or missing. Thus some improved Demons algorithms have been introduced [9], [10], [16]. Vercauteren et al. [22] have introduced an efficient second-order minimization [19] into Demons to improve the search direction of a Gauss-Newton-like method. On the other hand, it is widely acknowledged that the estimated transformation should be diffeomorphic and may thus preserve the topological structure that is important to such practical applications as computational anatomy. A way to resolve this issue is using B-splines [13] to get a sequence of diffeomorphic free-form deformations, but diffeomorphisms by spline transformation is hard to obtain for very large-deformation images. Next, large deformation diffeomorphic metric mapping (LDDMM) [14], [15] is proposed to find a time-dependent velocity field representation of diffeomorphism and shows high registration accuracy. Unfortunately, LDDMM is very time-consuming and highly memory-intensive since gradient optimization runs through the entire process of diffeomorphisms. Then, an efficient non-parametric diffeomorphic image registration algorithm, named Log-Demons [20], [21], is proposed, whose diffeomorphism is obtained by carrying out an optimization procedure on a Lie group. Log-Demons is attractive as its diffeomorphic mapping and computation is of linear complexity. And then, some Log-Demons based algorithms have been propsed to improve image registration performance [12], [31], [32], but they are hard to accurately acquire very large and complex deformations.

In most conventional methods for dealing with large deformations, a coarse-to-fine warping framework is used [5]. Yet it often leads gradient-based methods to local optima, even in coarse resolution [29]. To preserve details for large displacement, the studies propose to integrate descriptors into the variational optical flow [11], [17], [18]. However, many motion details are easy to miss and such transformations are not diffeomorphic because of the mismatching of feature points. Cifor et al. [27] propose a hybrid feature-based Log-Demons registration by combining a block-matching with Log-Demons. But it is difficult to deal with images with a complex

Manuscript received June 1, 2018; revised February 4, 2019; accepted June 10, 2019. Date of publication June 26, 2019; date of current version September 4, 2019. This work was supported in part by the National Nature Science Foundation of China under Grant 61773166 and Grant 61772369, in part by the Natural Science Foundation of Shanghai under Grant 17ZR1408200, in part by the Science and Technology Commission of Shanghai Municipality under Grant 14DZ2260800, in part by the Joint Funds of the National Science Foundation of China under Grant U18092006, in part by the Changjiang Scholars Program of China, Shanghai Science and Technology Committee, under Grant 17411953100 and Grant 16JC1401300, and in part by the Shanghai Municipal Science and Technology Committee of Shanghai Outstanding Academic Leaders Plan under Grant 19XD1434000. The associate editor coordinating the review of this manuscript and approving it for publication was Prof. Gene Cheung. *(Corresponding authors: LiangHua He; MengChu Zhou.)*

Y. Wen and L. Zhang are with the Department of Computer Science and Technology, East China Normal University, Shanghai 200062, China (e-mail: ywen@cs.ecnu.edu.cn).

L. He is with the Key Laboratory of Embedded System and Service Computing, Ministry of Education, Tongji University, Shanghai 200092, China (e-mail: helianghua@tongji.edu.cn).

M. Zhou is with the Department of Electrical and Computer Engineering, New Jersey Institute of Technology, Newark, NJ 07102 USA (e-mail: zhou@njit.edu).

This article has supplementary downloadable material available at http://ieeexplore.ieee.org, provided by the authors.

Digital Object Identifier 10.1109/TIP.2019.2924168

scenario. Lombaert et al. [28], [29] propose a spectral representation registration based on Log-Demons, which employs the spectral global matching to capture large deformations, but the cost of spectral matching is very high. To avoid the dependence on high descriptor matching accuracy, Lin [30] proposes a Mesh-based Photometric Alignment (MPA) method. It minimizes photometric errors on sampled points rather than feature correspondences to achieve a better global alignment. But when dealing with boundary points of an object, it may cause misalignment. In a word, the above methods cannot provide a well-satisfied performance for large-deformation image registration in such aspects as details-preserving, diffeomorphic deformation, and computational efficiency.

In order to tackle the above mentioned problems, we propose a structural Tensor and Driving force-based Log-Demons algorithm for large-deformation image registration, called TDLog-Demons. We utilize a driving force to capture large deformation, and a structural tensor to acquire an improved deformation field. To obtain smooth deformation, we use the structural tensor of an image as the constraint in registration. A tensor is a high-order extension of a matrix, and a second-order tensor describes the local structure of an image, e.g., lines and edges. Therefore, we extract the tensors of a fixed image and warped one, and take the tensor difference as a similarity criterion, which is added to Log-Demons to achieve smooth deformation. To capture large deformation, we introduce a driving force to tackle the local optimum problem faced by Log-Demons. We first use the Canny algorithm to extract images' boundary points as driving points, and then adopt Multisupport-Region-Order-based Gradient Histogram (MROGH) [25] descriptor to describe each driving point. The MROGH descriptor has an intrinsic rotation invariant and performs noticeably well in point matching and object recognition. Thus, it also well describes the characteristics of image boundary. The driving point's corresponding relations obtained by descriptor matching is considered as a driving force defined in this paper. Next, we integrate the driving force into Log-Demons. To achieve successful registration, we innovatively add a driving force to the velocity field rather than directly substituting displacement vectors with matching results [28] in each iteration.

Our main contributions include: 1) We propose to utilize a tensor conservation criterion to constrain the diffusion of pixels to obtain a desired local structure and smooth deformation. 2) We propose to apply a driving force obtained by boundary point correspondence to the update of Log-Demons in a global sense. The driving force in an exponentially decreasing form is integrated into the velocity field of Log-Demons to force points to move accuratly and to accelerate a registration process. 3) We carry out extensive experiments to demonstrate that our method has an excellent performance, especially for large-deformation image registration in comparison with the state-of-the-art methods.

The rest of the paper is organized as follows: The next section presents the Log-Demons method. Section III introduces the proposed method. The experimental results are presented in Section IV. Finally, conclusions are drawn in Section V.

II. Preliminary

In this section, we give a brief introduction to Demons and Log-Demons algorithms.

A. Definition of Registration Algorithm

Non-rigid registration algorithm aims at finding a well-behaved spatial transformation s that well aligns fixed image F and moving image M. We use $p \to s(p)$ to indicate that a point p in F is mapped to a point $s(p)$ in M by transformation. Generally, spatial transformation s is represented by a dense displacement vector. In case of small deformation, $p \to p + s(p)$. The similarity measure is established by using the difference between F and M, and an energy function of registration algorithm can be represented as:

$$E(s) = \frac{1}{\lambda_i^2} Sim(F, M \circ s) + \frac{1}{\lambda_T^2} Reg(s) \tag{1}$$

where parameter λ_i controls the consistency in intensity, and parameter λ_T controls the degree of regularization. Similarity criterion $Sim(F, M \circ s) = \|F - M \circ s\|^2$ is used to measure the resemblance of images, and "$\circ$" means the compositive adjustment. Regularization energy $Reg(s) = \|s\|^2$ is used as prior knowledge to obtain stable and smooth solutions.

B. Demons Algorithm

The Demons algorithm's concept stems from Maxwell's demons [38]. Thirion borrows the thoughts of a diffusion model to perform image-to-image matching. His main idea is to take the contour of the fixed image as a semi-permeable membranes that contain "demons", and take the moving image as a deformable grid. He determines whether or not the points in a grid can diffuse through a semi-permeable membrane, such that the points in the moving image can diffuse and finally two images achieve matching.

In order to cast the Demons into a problem to minimize a well-posed criterion, Cachier et al. [10] introduce a hidden variable c in a registration process. The idea is to consider c as an exact realization of the spatial transformation s, which allows some error at each image point. s should be close to the real one after smoothing. Thus the Demons algorithm is:

$$E(F, M, c, s) = \frac{1}{\lambda_i^2} Sim(F, M \circ c) + \frac{1}{\lambda_x^2} d(s, c)^2 + \frac{1}{\lambda_T^2} Reg(s) \tag{2}$$

where $d(s, c) = \|c - s\|$ estimates the difference between transformation s and c, and parameter λ_x represents the degree of uncertainty. The smaller λ_x, the larger the deformation.

By introducing the hidden variable c into the energy function, we can decouple the original optimization problem into two tractable sub-problems: (1) The optimization of $\frac{1}{\lambda_i^2} Sim(F, M \circ c) + \frac{1}{\lambda_x^2} d(s, c)^2$ to obtain c given s; and (2) The regularization by computing $\frac{1}{\lambda_x^2} d(s, c)^2 + \frac{1}{\lambda_T^2} Reg(s)$ to obtain s given c.

The first step is to solve an optimization problem. It should be noted that different optimization strategies lead to different expressions of a Demons force. A Gauss-Newton-like approach is often adopted, and the intensity difference $\varphi_p^s(\cdot)$ at point p is expressed as:

$$\begin{aligned}\varphi_p^s(u) &= F(p) - M \circ (s \circ u)(p) \\ &\approx \varphi_s^p(0) + J^p \cdot u(p) \\ &= F(p) - M \circ s(p) + J^p \cdot u(p)\end{aligned} \tag{3}$$

where gradient J^p is defined as $J^p = \nabla M \circ s(u)$. u stands for the updated field in each iteration. Transformation s can be calculated as $s = s \circ u$. Thus, the Demons can be rewritten as:

$$E_s'(u) \approx \frac{1}{2|\Omega_p|} \sum\nolimits_{p \in \Omega_p} \left\| \begin{bmatrix} F(p) - M \circ s(p) \\ 0 \end{bmatrix} + \begin{bmatrix} J^p \\ \frac{\lambda_i(p)}{\lambda_x} I_E \end{bmatrix} \cdot u(p) \right\|^2 \tag{4}$$

where Ω_p stands for the overlap between F and $M \circ s$ and I_E represents an identity matrix. It is noted that $E_s'(u)$ means the energy of the first step of Log-Demons, while $E(u)$ means the whole energy of Log-Demons. After the optimization, we can obtain the updated field u for each pixel p:

$$u(p) = -\frac{F(p) - M \circ s(p)}{\|J^p\|^2 + \frac{\lambda_i^2(p)}{\lambda_x^2}} J^p \tag{5}$$

The second step is usually used to smooth the updated field u by using Gaussian kernels K_1 and K_2 with standard deviations σ_1 and σ_2, respectively.

C. Log-Demons Algorithm

In such applications as medical image registration or registration-based target segmentation and recognition, the resulting deformation field often requires good continuity, smoothness, and diffeomorphism. Diffeomorphism is a continuous reversible smooth mapping and its inverse mapping is also smooth. In order to perform diffeomorphic image registration, Vercauteren et al. [20] propose a Log-Demons algorithm. It utilizes a Lie group structure to obtain diffeomorphic transformation s, by using an exponential mapping of a velocity field υ, $s = \exp(\upsilon)$. The exponential mapping can be quickly calculated with a scaling and squaring method by using multiple first-order integrals of all pixels in the updated field to accelerate its computation. (Details are shown in Algorithm 1 in Supplementary File.)

At each iteration, Log-Demons looks for the updated field u in the Lie algebra, and then maps it in the space of diffeomorphism via exponential mapping. Hence, the updated step is in the form of $s = s \circ \exp(u)$. The energy function of Log-Demons is:

$$E(u) = \frac{1}{\lambda_i^2} Sim(F, M \circ s \circ \exp(u)) + \frac{1}{\lambda_x^2} dist(s, s \circ \exp(u))^2 + \frac{1}{\lambda_T^2} Reg(s) \tag{6}$$

Through its optimization, we can obtain the same updated field with Demons. The difference lies in that the updated method of Log-Demons is $s = s \circ \exp(u)$ but not $s = s \circ u$, where u stands for a speed vector field in Log-Demons but not a dense displacement field in Demons. Note that Log-Demons is realized in Algorithm 2 in Supplementary File.

III. PROPOSED TDLOG-DEMONS

We propose a structural Tensor and Driving force-based Log-Demons algorithm for large-deformation image registration, called TDLog-Demons for short. TDLog-Demons includes four parts: similarity criteria based on a driving force, similarity criteria based on tensor consistency, transformation difference and regularization. We integrate a structure tensor and a driving force into the model of Log-Demons next.

A. Log-Demons With Structural Tensor

Structural tensors have a wide range of applications in image enhancement and image restoration, as first defined by Zenzo [37]. It has a good adaptability to illumination changes, and can extract more local structural information of an image, even when the local gradient of an image is missing.

For a two-dimensional image I, the gradient is: $\nabla I = [I_x, I_y]^T$, where $I_x = \frac{\partial I}{\partial x}$ and $I_y = \frac{\partial I}{\partial y}$ represent the horizontal and vertical gradients, respectively. The structural tensor of an image is:

$$I_T = (\nabla I)^T (\nabla I) = \begin{bmatrix} I_x^2 & I_x I_y \\ I_x I_y & I_y^2 \end{bmatrix} \tag{7}$$

Since (7) is only a symmetric matrix generated by the gradient information in the image, it is sensitive to the noise and cannot reflect the structural information of an image perfectly. Therefore, a Gaussian filter should be added to (7). Suppose that G_σ is the kernel function of a Gaussian filter. The structural tensor is rewritten as:

$$I_T = G_\sigma * (\nabla I)^T (\nabla I) = \begin{bmatrix} I_x^2 G_\sigma & I_x I_y G_\sigma \\ I_x I_y G_\sigma & I_y^2 G_\sigma \end{bmatrix} \tag{8}$$

A tensor is represented as a matrix, which can be calculated by using eigenvalues and their corresponding eigenvectors. Assuming that the eigenvalues of image tensor I_T are λ_1 and λ_2 respectively, with eigenvectors r_1 and r_2. Thus, we obtain the trace $Tr(I_T)$, which indicates the strength of the tensor:

$$Tr(I_T) = G_\sigma * (I_x^2 + I_y^2) = \lambda_1 + \lambda_2 \tag{9}$$

In order to improve the accuracy and smoothness of registration, we combine the structural tensor with Log-Demons to construct a new registration energy expression. Our main idea is that the difference between the warped and fixed images should be as small as possible, and the structural tensor of images should be consistent:

$$\begin{aligned}E(u) = &\frac{1}{\lambda_i^2} Sim(F, M \circ s \circ \exp(u))) \\ &+ \frac{1}{\lambda_j^2} Sim(Tr(F_T), Tr((M \circ s \circ \exp(u))_T) \\ &+ \frac{1}{\lambda_x^2} dist(s, s \circ \exp(u)))^2 + \frac{1}{\lambda_T^2} Reg(s)\end{aligned} \tag{10}$$

where F_T and $(M \circ s \circ \exp(u))_T$ represent the structural tensor of fixed and warped images, respectively, and λ_j controls the

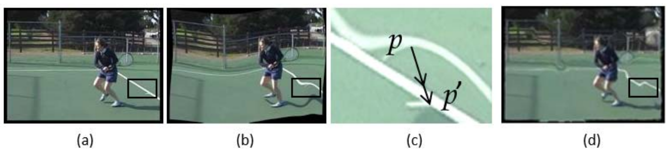

Fig. 1. The sketch of the driving force of two corresponding boundary points. (a) Fixed image. (b) Moving image. (c) The correspondence of p and p'. (d) The registration result of Log-Demons.

effect of the structural tensor on Log-Demons. $E(u)$ in (10) is optimized in a manner similar to Log-Demons, and the updated field can be calculated as:

$$u(p)=-\frac{F(p)-M\circ s(p)}{\|J^P\|^2+\frac{\lambda_i^2(p)}{\lambda_x^2}}J^p-\frac{|F(p)-M\circ s(p)|}{\|K^p\|^2+\frac{\lambda_j^2(p)}{\lambda_x^2}}K^p \quad (11)$$

where $K^p = \nabla(Tr(F_T - M\circ s(p)))$. The proposed new updated field not only takes the gray scale gradient information into account, but also retains the local structural features. The optimization process of Log-Demons with a structural tensor is similar to that of Log-Demons. It has two steps: (a) calculate the updated speed field according to (11), and (b) regularize the updated field.

B. Log-Demons With Driving Force

We begin with our discussion about how to deal with very large deformation. Since the gradient computation may fall into local optima, many gradient-based registration methods are hard to capture very large deformations. A popular solution is to establish accurate pointwise correspondence via a feature matching technique [29] so as to drive the movements of points globally. Log-Demons can not well match images with very large deformations such as severe image distortion because it is hard to match their boundaries precisely. The Demons force relies on the difference between F and M, while excessive deformation may cause non-overlap, thus easily leading to a wrong direction of diffusion. Since the image boundaries are rich in details and vital to diffusing models of Demons, we plan to find the boundary point correspondence of two images and take such correspondence as a driving force. In this paper, we propose to apply a Canny detector to extract image boundary points as driving points and seek the correspondence between driving points of two images as a driving force. The Demons force is integrated with a driving force to push the points to move together. As a result, such integration is able to produce a more precise registration. For example, Figs. 1(a)-(b) are F and M, respectively. Fig. 1(c) gives the sketch of the driving force of two corresponding boundary points. If the registration method could push the movement of point p' along the correct direction to point p, the result would be correct. However, Log-Demons fail to get the satisfactory result shown in Fig. 1(d). Thus a driving force integrated into the Demons force is proposed, to guide p' to move as indicated by the black arrows in Fig. 1(c).

We face two issues: how to integrate a driving force into Log-Demons and how to compute it. We first explain the function of Log-Demons with a driving force. M and F are a moving image and a fixed one, respectively. We can calculate the driving force u^c between M and F and then integrate it into the continuous optimization of Log-Demons. In order to integrate the updated field u and driving force u^c to obtain diffeomorphism, we perform exponential mapping on the latter. We calculate u^c in the Lie Algebra, and then map it to a Lie group. Thus, we derive the energy function of Log-Demons with driving force as follows:

$$\begin{aligned} E(u) = &\frac{1}{\lambda_i^2}Sim(F, M\circ s\circ \exp(u)\circ\exp(\frac{1}{\lambda_k^2}u^c)) \\ &+\frac{1}{\lambda_x^2}dist(s, s\circ\exp(u)\circ\exp(\frac{1}{\lambda_k^2}u^c))^2 \\ &+\frac{1}{\lambda_T^2}Reg(s) \end{aligned} \quad (12)$$

In Eq.(12), the driving force u^c is integrated to the Demons force. λ_k controls its influence on the updated field u and is set as $\lambda_k = 2^{(k-1)/2}, k = 1, 2, \ldots, 100$, where k is the iteration count in Log-Demons. When k is small, $\exp(u^c/{\lambda_k}^2)$ is big, but $\exp(u^c/{\lambda_k}^2)$ reduces as k increases. Thus, a driving force is strong on the diffusion at the beginning and decreases rapidly as iterations proceed. Instead of directly replacing the updated field by the driving force, we have adopted a fusion way. The driving force u^c leads to the global optimization of Log-Demons since u^c can drive points to diffuse towards a right direction rapidly and accurately, when descriptor matching has high accuracy in a global space.

To optimize (12), according to the Baker-Campbell-Hausdorff (BCH) formula [21], we have:

$$\exp(Z(u, \frac{1}{\lambda_k^2}u^c)) \approx \exp(u)\circ\exp(\frac{1}{\lambda_k^2}u^c) \quad (13)$$

where $Z(\cdot)$ can be expressed as the Lie bracket:

$$\begin{aligned} \exp(Z(u, \frac{1}{\lambda_k^2}u^c)) = &u + \frac{1}{\lambda_k^2}u^c + \frac{1}{2}[u, \frac{1}{\lambda_k^2}u^c] \\ &+\frac{1}{12}[u,[u,\frac{1}{\lambda_k^2}u^c]] + O(\left\|\frac{1}{\lambda_k^2}u^c\right\|^2) \end{aligned} \quad (14)$$

Vercauteren et al. [21] have verified that $Z(\cdot)$ can be approximated with high accuracy. In order to compute it simply, we replace (13) with $\exp(Z(u, \frac{1}{\lambda_k^2}u^c)) \approx u + \frac{1}{\lambda_k^2}u^c$. Through the first order expansion of intensity difference in the first step of Log-Demons:

$$F(p)-M\circ s\circ\exp(Z)(p)\approx F(p)-M\circ s(p)+J^pZ(p) \quad (15)$$

Distance between two diffeomorphisms is approximated as:

$$d(s, s\circ\exp(Z)) \approx \|u\| \quad (16)$$

The energy function of the first step of Log-Demons can be rewritten as:

$$\begin{aligned} E_s'(u) \approx \frac{1}{2|\Omega_p|}\sum_{p\in\Omega_p}\Bigg\|&\begin{bmatrix} F(p)-M\circ s(p) \\ 0 \end{bmatrix} \\ &+\begin{bmatrix} J(p) \\ \frac{\lambda_i(p)}{\lambda_p}I_E \end{bmatrix} Z(u,u^c)\Bigg\|^2 \end{aligned} \quad (17)$$

where Ω_x is the overlap between F and $M \circ s$. By minimizing the energy in (17), at each pixel p, we can obtain

$$u(p) = -\frac{|F(p) - M \circ s(p)|}{\|J^p\|^2 + \frac{\lambda_i^2(p)}{\lambda_x^2}} J^p - \frac{1}{\lambda_k^2} u^c \tag{18}$$

Thus, $u(p)$ is the updated field.

The Log-Demons with a driving force registration is implemented in Algorithm 3 shown in Supplementary File.

Second, we present a method to compute a driving force. We obtain driving points by using a Canny detector on M and F and employ a feature descriptor to describe the characteristics of driving points. In our method, the driving force u^c is defined as the correspondence among boundary points in two images, which can be obtained via descriptor matching. u^c can push points' direction of gradient descent in the process of calculating updated field u. Although there exist some good feature descriptors, such as SIFT [23], DAISY [24] and HOG [26], they need to assign a reference orientation for each point which may be a major error source for most of the existing methods [25]. Here, we select MROGH [25] to perform descriptor matching for large-deformation images because of its intrinsic rotation invariant and excellent performance in finding corresponding points with large orientation changed.

MROGH forms an inherent rotation invariance by constructing its own coordinate system for each point in the detected feature area. It can thus maintain great matching performance under large angle changes caused by large deformation. It uses a Harris-Affine detector to detect elliptical regions, and then these regions are normalized to canonical regions respectively as support regions. For each support region, all pixels are sorted in non-descending order by their grayscale value, and then they are divided equally to k groups. Each point in a support region is connected to the center point to form a coordinate system. Hence, gradient magnitude and orientation can be calculated and transformed to a d-dimensional vector. By directly adding the d-dimensional vectors of each pixel of each group in the support region, we can get k sets of d-dimensional vectors. Through superimposing these vectors in turn, the descriptor for a support region is obtained. In order to get more regional information to reduce mismatches, N regions are constructed by fixing the radius of expansion on the basis of a single support region, and the descriptors are constructed in the same way in these regions. N descriptors are connected to form a region descriptor, called Multisupport-Region-Order-Based Gradient Histogram (MROGH). The detailed calculation process is shown in Supplementary File.

After we calculate a descriptor for every driving point, for point x_i in M, we must find its corresponding point x_j in F via MROGH descriptor matching, as shown in Fig. 2. At the same time, x_j in F has its own corresponding MROGH descriptor matching point x_i' in M. If $x_i = x_i'$, we call x_i and x_j the mutually optimal corresponding points (red and blue points shown in Fig. 2(c)). Also, if $x_i = x_i'$, the displacement vector of x_i is obtained as $u_i^c = x_j - x_i$; otherwise $u_i^c = 0$. Note that u_i^c marked by a green arrow in Fig. 2(c) is the driving force in this work.

(a) Fixed Image (F) (b) Moving Image (M) (c) Driving Force

Fig. 2. Example of a driving force. (a) Fixed image (b) Moving image (c) Driving force.

C. Structural Tensor and Driving Force-Based Log-Demons

We propose a Log-Demons algorithm based on a structural tensor and driving force for large-deformation image registration. We use the former to preserve a local structure and obtain smooth deformation when deformation is small. Because of the defects of gradient-based methods, Log-Demons may be limited by a local space such that it fails to adapt to large deformation. To address this challenging issue, we propose to utilize a driving force to improve the diffusion process. Such force gives a great influence on the diffusion at the beginning, and decreases rapidly as the number of iterations grows. By combining a structural tensor and driving force with the model of Log-Demons, we propose TDLog-Demons as a new frame-work to perform large-deformation image registration. At the beginning of registration, a driving force plays a dominant role in dealing with large deformation. When the deformation becomes small, a structural tensor plays an important role to obtain smooth deformation. We thus define the energy function of TDLog-Demons as follows:

$$\begin{aligned} E(u) = {} & \frac{1}{\lambda_i^2} Sim(F, M \circ s \circ (\exp(u) \circ \exp(\frac{1}{\lambda_k^2} u^c))) \\ & + \frac{1}{\lambda_j^2} Sim(Tr(F_T), Tr((M \circ s \circ \exp(u))_T) \\ & + \frac{1}{\lambda_x^2} d(s, s \circ (\exp(u) \circ \exp(\frac{1}{\lambda_k^2} u^c)))^2 \\ & + \frac{1}{\lambda_T^2} Reg(s) \end{aligned} \tag{19}$$

After optimizing $E(u)$ in (25), the updated field of TDLog-Demons is:

$$\begin{aligned} u(p) = {} & -\frac{F(p) - M \circ s(p)}{\|J(p)\|^2 + \frac{\lambda_i^2(p)}{\lambda_x^2}} J(p) - \frac{1}{\lambda_k^2} u^c \\ & - \frac{|F(p) - M \circ s(p)|}{\|K(p)\|^2 + \frac{\lambda_j^2(p)}{\lambda_x^2}} K(p) \end{aligned} \tag{20}$$

In this way, not only can the proposed method adapt to large deformation during an image registration process, but also obtain an excellent deformation field and local structure. Next, we perform a number of experiments to evaluate the new framework.

IV. Experiments

A. Experiments of Structural Tensor

In this section, we perform experiments on synthetic and brain images respectively, to verify the effect of a tensor on

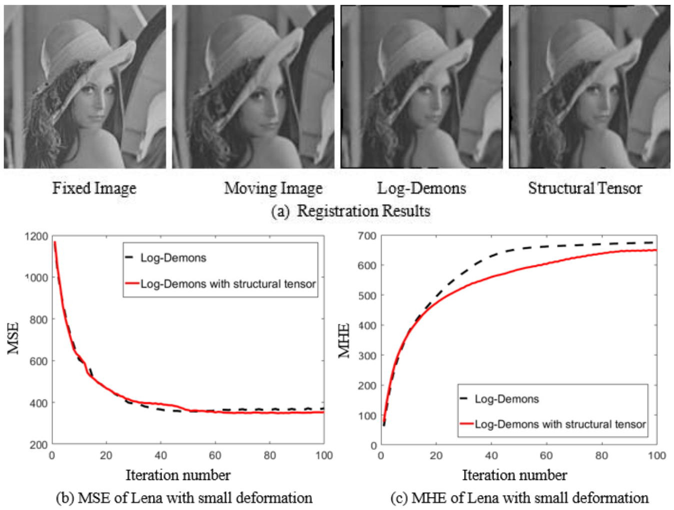

Fig. 3. Registration results of Lena with small deformation. (a) Registration results. (b) MSE of Lena with small deformation. (c) MHE of Lena with small deformation.

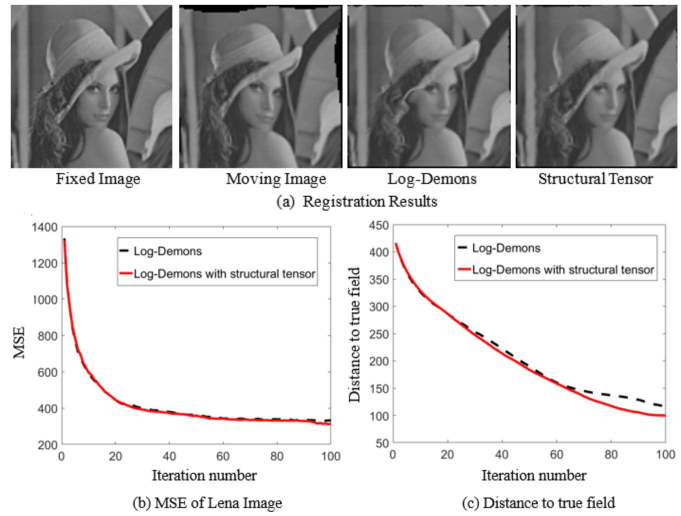

Fig. 4. MSE and distance to the true field of Lena. (a) Registration results. (b) MSE of Lena image. (c) Distance to true field.

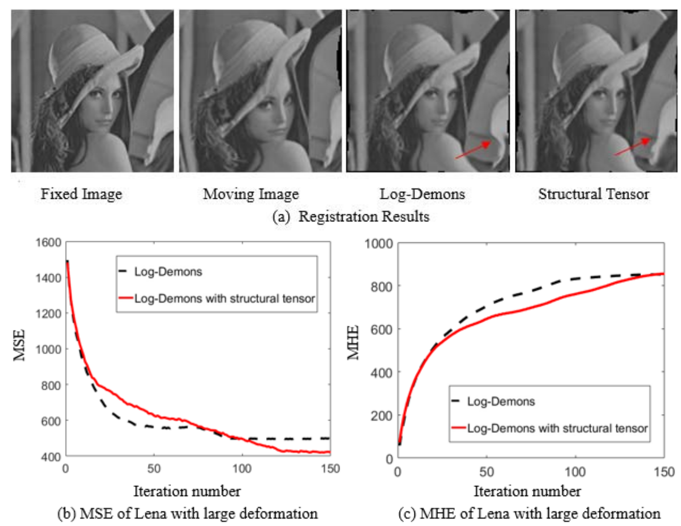

Fig. 5. Registration results of Lena with large deformation. (a) Registration rosults. (b) MSE of Lena with large deformation. (c) MHE of Lena with large deformation.

Log-Demons. In order to better assess the registration results, we use Mean Square Errors (MSE) and Mean Harmonic Energy (MHE) as the evaluation criteria.

$$MSE = \sqrt{\sum_{x=0}^{N-1} \sum_{y=0}^{N-1} (F(x, y) - M \circ s(x, y))^2} \quad (21)$$

$$MHE = \sqrt{\sum_{x=0}^{N-1} \sum_{y=0}^{N-1} (s(x, y))^2} \quad (22)$$

where F stands for a fixed image and M stands for a moving image, and s stands for a deformation field.

The former evaluates the differences in gray scale between fixed and warped images; while the latter calculates the deformation energy of a deformation field. MSE is the primary criterion and should be as small as possible. MHE grows as the deformation increases. When MSE is at the similar scale, the smaller MHE, the better, which means that it takes less energy to achieve the same effect. In order to compare our method with other algorithms under the same condition, we use the same parameters as other methods. The parameters in the expriments are definded as: $\lambda_i = 1$; $\lambda_j^2 = 2$; $\lambda_x = 2$; $\lambda_T = 1$; $K_1 = 1$; and $K_2 = 1$.

First, we verify the performance of the proposed algorithm in the case of small deformation. We randomly deform the classic Lena image with size of 128×128, using a smooth displacement field with a Markov random field sampler as described in [20], and the maximum deformation is 10 pixels. The registration results are shown in Fig. 3(a): The first image is a fixed one, and the second one is a moving one, and the third and fourth images are registration results of Log-Demons and Log-Demons with structural tensor, respectively. From registration results, we can see that both can finish registration well in case of small deformation, and the visual difference is small. MSE and MHE are shown in Figs. 3(b)-(c) respectively. Although the MSE curves of two algorithms are close, the final MSE of Log-Demons is 371.8, while Log-Demons with structural tensor is 353.3. The accuracy of the proposed method is clearly higher than that of Log-Demons. As shown in Fig. 3(c), the MHE of Log-Demons with structural tensor is consistently below that of Log-Demons, indicating that the proposed one requires less deformation energy than Log-Demons and thus yields a smoother deformation field.

We present MSE and distance to a true field with Log-Demons and our method in Fig. 4. We deform Lena with a random diffeomorphic deformation $s_t = exp(v)$ where v is random smooth deformation. The corresponding true field is defined as the inverse of the deformation $s_t{}^{-1} = exp(-v)$. Hence, the distance to the true field in each iteration is $\|M \circ s \circ exp(u) - s_t{}^{-1}\|^2$, where s is current deformation from moving image to fixed one and u is an updated field. It can be seen that although MSE of both methods are close (Fig. 4(b)), the distance to the true field with ours is closer than Log-Demons (Fig. 4(c)), thereby implying better performance.

We also perform experiments on a large-deformation image, and the maximum deformation is 20 pixels. From Fig. 5(a),

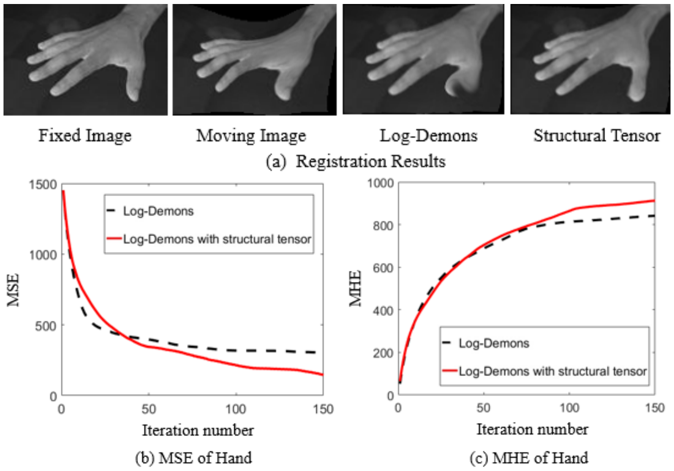

Fig. 6. Registration results of Hand. (a) Registration results. (b) MSE of Hand. (c) MHE of Hand.

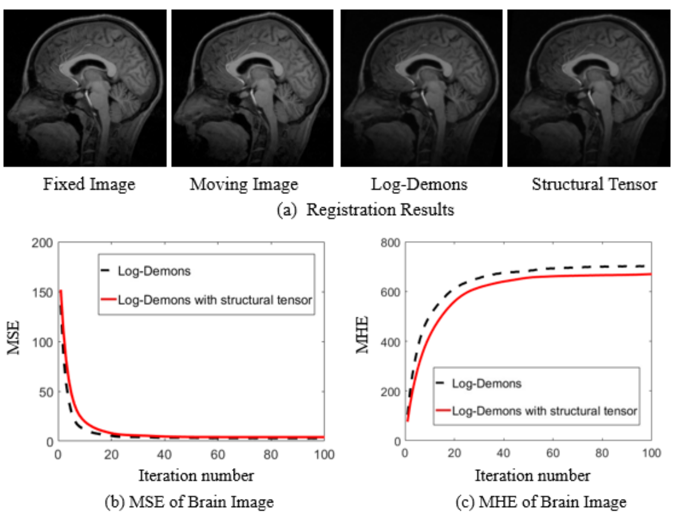

Fig. 7. Registration results of Brain Image. (a) Registration results. (b) MSE of brain image. (c) MHE of brain image.

we can see that Log-Demons fails to register them completely as shown by red arrows, while ours performs well. The registration accuracy of the algorithm can be observed via their MSE curves, in which the final MSE of Log-Demons with structural tensor is 421.5 while that of Log-Demons is 497.8.

In order to further evaluate the performance of the algorithm, we choose the simple Hand image to carry out the experiment. As shown in Fig. 6(a), the fixed image has a simple background. Log-Demons fails to complete the registration at the part of the thumb, while the proposed method has a better result, which can also be clearly seen from their MSE values.

We test the algorithm on a brain image registration, and the results are shown in Fig. 7. The registration results and MSE curves are close, while MHE of ours is much better than that of Log-Demons. It is shown that the deformation field obtained by our method is more accurate and the energy consumption is smaller. In conclusion, a structural tensor has a positive effect on Log-Demons and leads to a smoother registration process.

B. Experiments of TDLog-Demons and Its Peers

In this subsection, we carry out experiments on three types of images, i.e., synthetic images, real scene images and brain images to validate the performance of TDLog-Demons. We compare TDLog-Demons with some popular registration algorithms, such as Log-Demons, Spectral Log-Demons and LDDMM. We use the default parameters of the three methods. The parameters of the proposed method in the following experiments are the same as that of the previous experiment. MSE is used to evaluate the intensity difference between fixed and warped images.

1) Large-Deformation Image Registration Experiment on Synthetic Images: In this experiment, we deal with image registration with very large deformations. The moving images are all synthetic ones. Let $\lambda_x = 2$. All the tested methods have converged after performing 100 iterations through the experiment. We select five fixed images and warp them with randomly large deformations, and Fig. 8 shows the final registration results. The first image of each row is a fixed one and the second one is a deformed moving one, followed by the registration results of Log-Demons, LDDMM, Spectral Log-Demons, and TDLog-Demons.

In Fig. 8, in the examples of Tennis and Marble, twisted line matching is a difficult task for all existing registration methods. For example, the railings in Tennis are aligned incorrectly by its three peers since the lack of an external force pushes them to align with the corresponding lines. Our method restores the lines successfully. For Shoes and Football, the texture in these two images is rich and our method has achieved good registration results. For Mountain and Temple, there exist not only overall distortion but also local large deformation. TDLog-Demons and spectral Log-Demons yield better results than the other two. TDLog-Demons has the lowest MSE among all tested methods. The above examples demonstrate that the driving force obtained by boundary point correspondence can restrain the movement of points and is vital to keep complete object outline and details in the process of registration.

The MSE curves of Spectral Log-Demons, Log-Demons, LDDMM and TDLog-Demons are plotted in Fig. 9. For these experiments, except Football and Mountain, MSE curve of TDLog-Demons drops the fastest and is nearly always below those of its peers, indicating that TDLog-Demons registers images effectively and accurately. Exceptions occur for Football and Mountain that exhibit lots of local deformations. Because of mismatches of descriptors, the driving force may have negative influence on the Demons force, thus slowing down the convergence of TDLog-Demons. It can be seen that the matching accuracy of descriptors plays a key role in large-deformation image registration. More illustrations are shown in Supplementary File.

In order to detail the process of registration, we choose Heart to show intensity differences of different registration methods. The colormaps transformed by the intensity differences of warped images are shown in Fig. 10, in which blue color means no difference and red color means that intensity difference is the biggest. From top to bottom, the

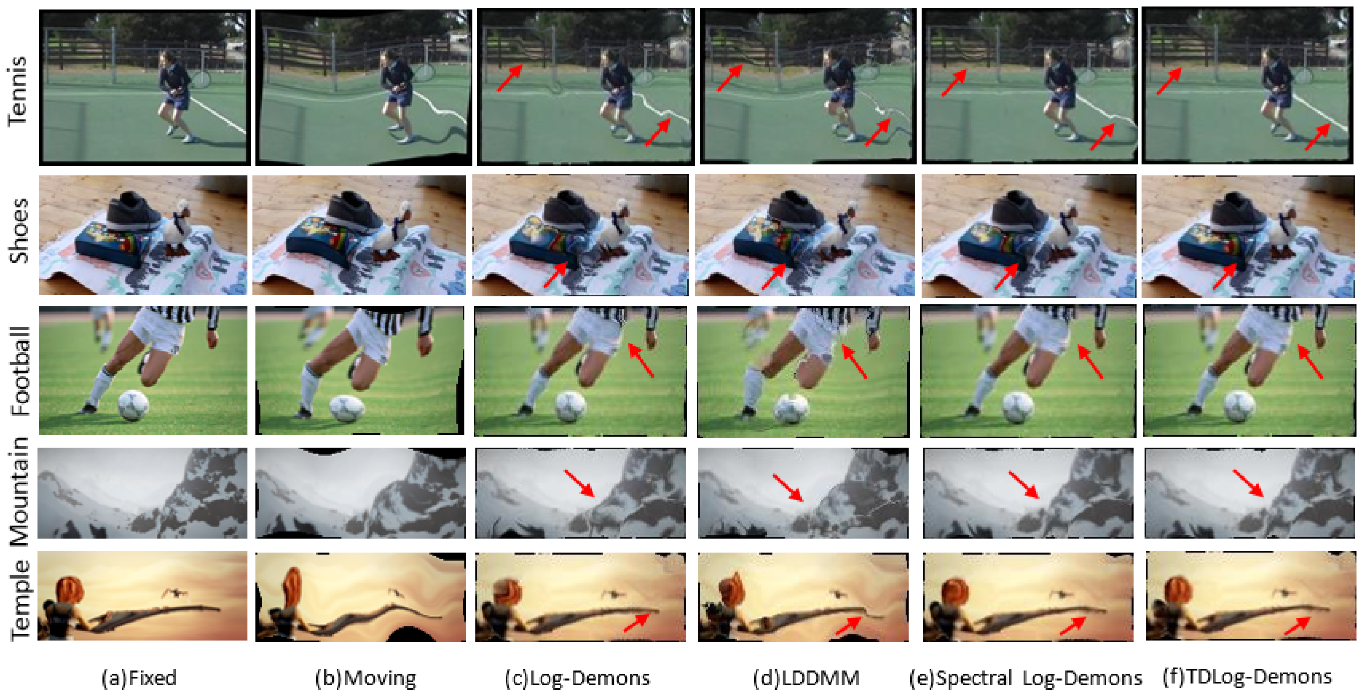

Fig. 8. The synthetic images' registration results of different methods. From top to bottom, the names and size of images are Tennis(185 × 135), Shoes(200 × 110), Football(135 × 80), Mountain(145 × 60) and Temple(135 × 60). And from left to right, images of each row are (a) fixed image, (b) moving image, registration results of (c) Log-Demons, (d) LDDMM, (e) Spectral Log-Demons and (f) TDLog-Demons respectively.

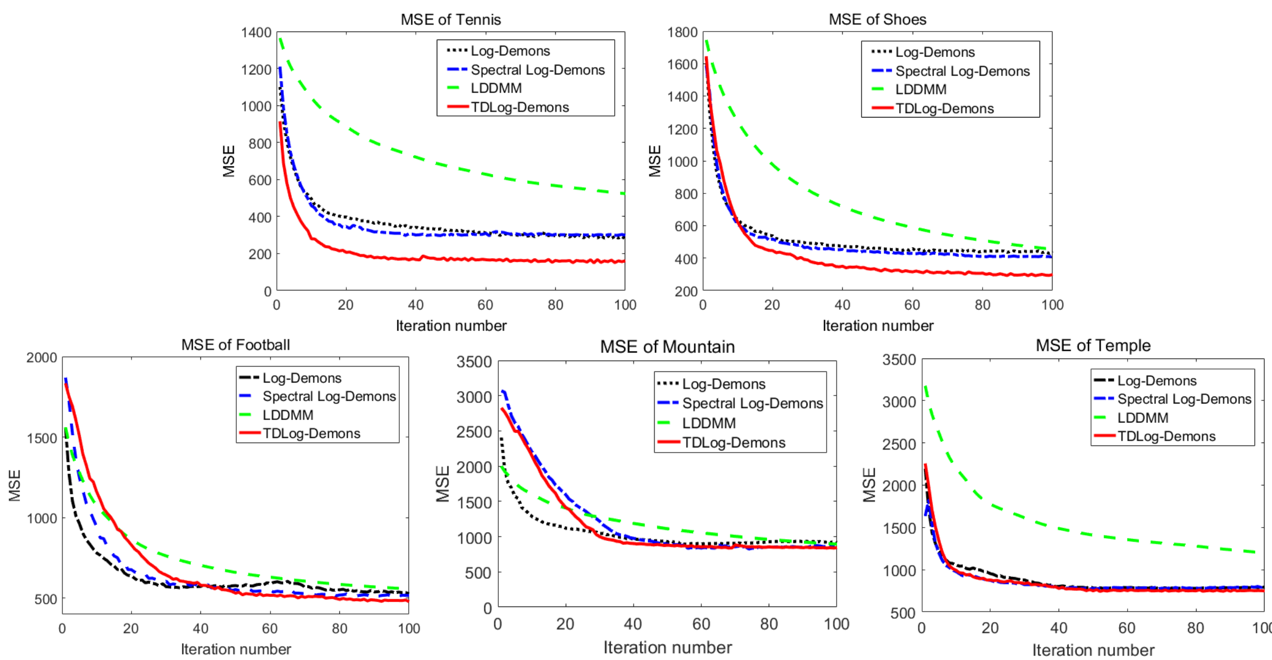

Fig. 9. MSE curves of different registration methods, the blue, black, green and red curves stand for Spectral Log-Demons, Log-Demons, LDDMM and TDLog-Demons, respectively.

colormaps are obtained by Log-Demons, LDDMM, Spectral Log-Demons and TDLog-Demons respectively when iteration count is 1, 5, 10, 20 and 100. In the first 10 iterations, the proposed method can nearly correctly restore Heart while its three peers fail. Fig. 10 demonstrates that the driving force should have a very big impact on Log-Demons at the beginning, and declines its impact as the intensity difference reduces.

2) Deformation Scale Experiment: In order to investigate the registration performance of each algorithm at different deformation scales, we randomly deform the Lena's picture with the maximum deformations being 5, 10,…, and 40 pixels respectively. The registration results are shown in Fig. 11. Fig. 11(a) presents the MSE at different scales, in which line Controls stands for MSE between fixed and moving images, and other curves represent MSE curves of four methods.

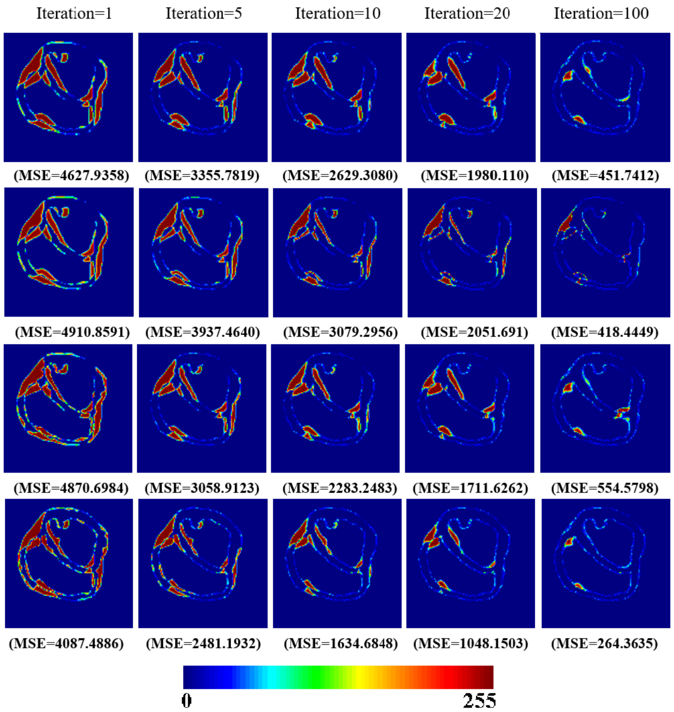

Fig. 10. The colormaps of intensity difference for Heart. From top to bottom, the colormaps are obtained by Log-Demons, LDDMM, Spectral Log-Demons and TDLog-Demons respectively when iteration count is 1, 5, 10, 20 and 100.

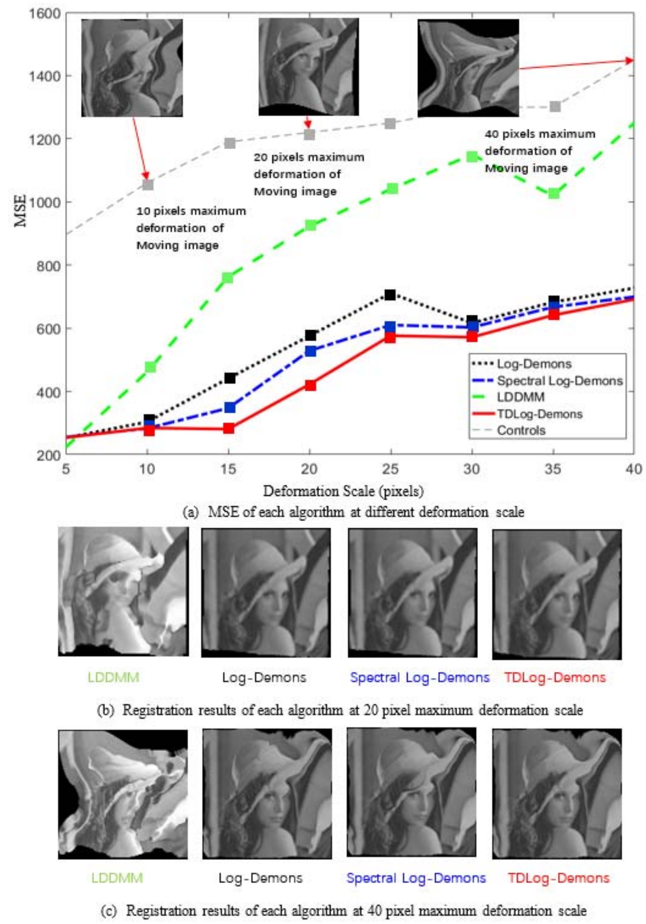

Fig. 11. Deformation scale experiment. (a) MSE of each algorithm at different deformation scale. (b) Registration results of each algorithm at 20 pixel maximum deformation scale. (c) Registration results of each algorithm at 40 pixel maximum deformation scale.

The three images are moving images with the deformations 10, 20, and 40 pixels, respectively. Figs. 11(b) and (c) show the registration results of four algorithms at 20 and 40 pixels deformations, respectively. We conclude that all have great performance when deformation scale is small, i.e., less than 10 pixels. When it increases, the moving images present larger and larger deformation. When it is between 20 to 30 pixels, the registration result using TDLog-Demons is still better than its peers. When the deformation scale is over 35 pixels, it is difficult for all registration methods to perform well, while MSE of TDLog-Demons is clearly lower than those of other algorithms. However, when the scale is over 40 pixels, all methods fail to register successfully.

3) Effect of Structural Tensor on Log-Demons With Driving Force: In this experiment, we verify the effect of a structural tensor on Log-Demons with a driving force [39]. We randomly deform Lena, and the maximum deformations are 5, 15 and 25 pixels respectively. Figs. 12(a)-(c) present MSE curves, Figs. 12(d)-(f) present the corresponding MHE curves and Figs. 12(g)-(i) show the distance to the true field. The MSE of Log-Demons with a driving force and TDLog-Demons are very close. The final MSE of Log-Demons with a driving force in each deformation scale is 49.41, 258.80, 527.70, 775.63, and 1981.20, while the corresponding ones of TDLog-Demons are 49.00, 266.71, 500.21, 789.73, and 1906.40. It can be seen that the structural tensor alone has limited impact on MSE reduction. According to MHE and distance curves, TDLog-Demons has a significant reduction compared with Log-Demons with a driving force. Especially as iterations proceed, MHE differences become more pronounced. As the deformation increases, its advantage in terms of distance to the true field becomes clearer and clearer. The results suggest that when the deformation becomes small, the structural tensor has a clearly positive effect, which can promote Log-Demons with a driving force to better deal with the larger deformation. We can conclude that the driving force helps Log-Demons capture large deformation, when the deformation becomes small and the influence of the driving force is weakened, while the structural tensor plays a relatively larger role to obtain better registration.

C. Experiments on Real Images

Brox dataset [17] and MIT dataset [35] are two datasets containing real scene sequences. Their images contain occlusion and large displacement. In this experiment, we randomly choose some sequences from two datasets to investigate the performance of the proposed TDLog-Demons and its peers. This experiment uses a coarse-to-fine strategy and is conducted in four levels. The deformation s calculated in lower resolution is taken as the initial value to perform the next higher resolution level registration, which can accelerate the computation. Some images and registration results are presented in Fig. 13.

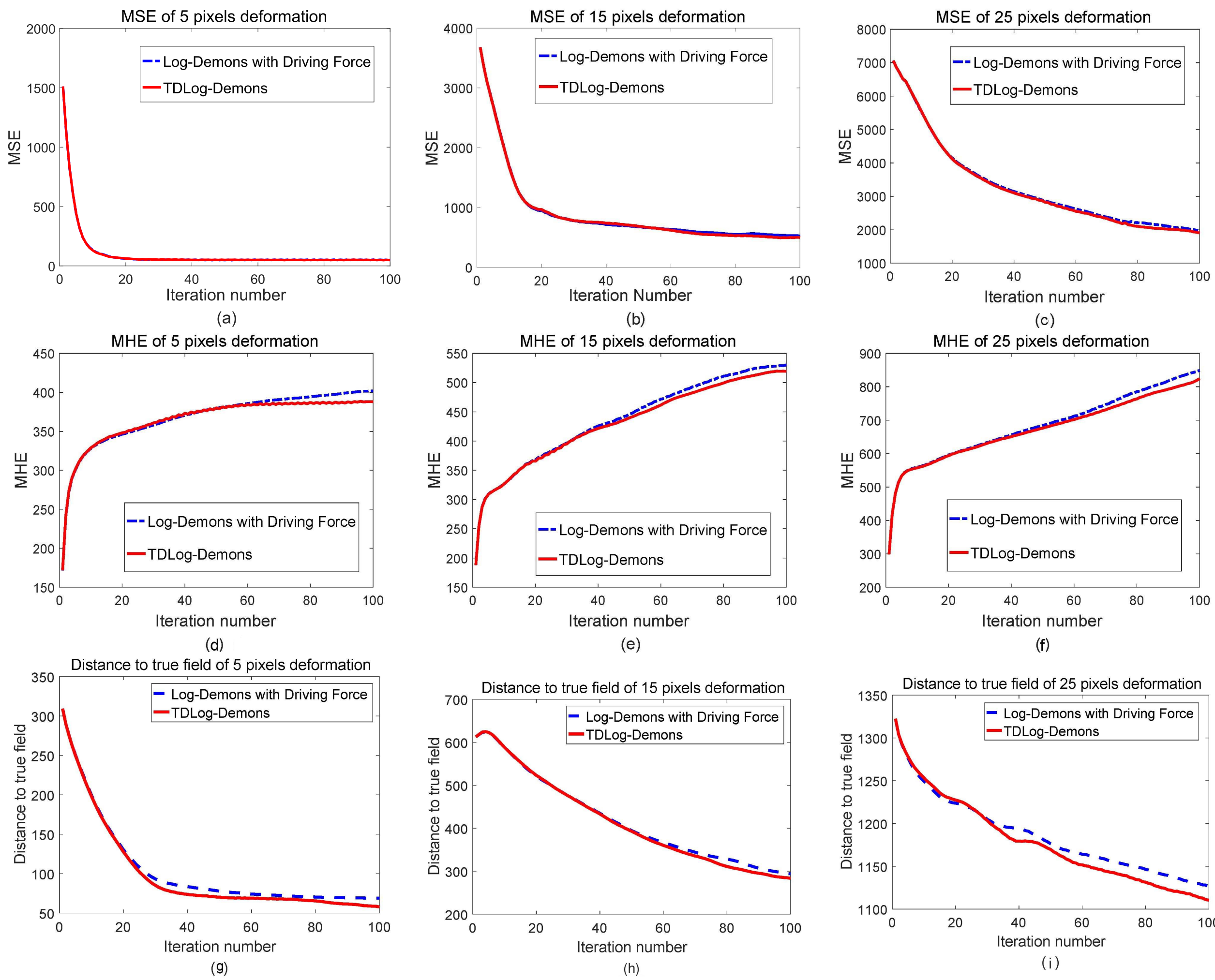

Fig. 12. Comparison between Log-Demons with driving force and TDLog-Demons when random deformations are 5,15 and 25 pixels, respectively.

TABLE I
MSE AND STANDARD DEVIATION OF FIVE METHODS ON REAL SCENE SEQUENCES

Mean MSE	Log-Demons	LDDMM	Spectral Log-Demons	Log-Demons with driving force	TDLog-Demons
Tennis	125.78(±9.22)	210.79(±14.65)	126.13(±8.54)	126.05(±12.16)	126.17(±12.19)
Marple	174.23(±55.98)	783.91(±59.02)	204.62(±54.26)	167.16(±37.07)	165.42(±49.34)
BirdHouse	450.60(±45.25)	413.75(±48.19)	450.84(±33.27)	436.79(±36.86)	423.11(±38.02)
Fish	116.46(±38.37)	197.89(±41.33)	104.13(±32.65)	109.12(±35.66)	106.87(±21.54)

The first image of each row is a fixed image and the second image is a moving one, followed by the registration results of four methods. As shown in Fig. 13, all final registration results are very close in vision, but the proposed method achieves good results. Furthermore, we randomly select 10 images from each sequence to get the mean and standard deviation of MSE of different methods, shown in Table I. It is clear that our method on a real scene sequence has its performance advantages, and the structural tensor and driving force integrated into Log-Demons can lead to a consistently precise result. The results about other sequences are detailed in Supplementary File.

In addition, we experimentally investigate the performance of the proposed method on MR brain image registration. We randomly select 35 T1 images [33] for evaluation. These brains are differentiated by their morphology. We also conduct the experiment in four levels.

To compare the registration accuracy, a brain image by using the method of FMRIB Software Library [36] is segmented into three tissues: white matter (WM), gray matter (GM), and cerebrospinal fluid (CSF). Then, we adopt MSE and Dice coefficient (DC) [34] to estimate the accuracy. The function of DC is:

$$DC = 2 * \frac{|O^F \cap O^W|}{|O^F| + |O^W|} \tag{23}$$

where F and W stand for fixed and warped images, and O^F and O^W stand for the number of pixels in WM, GM, and CSF, respectively.

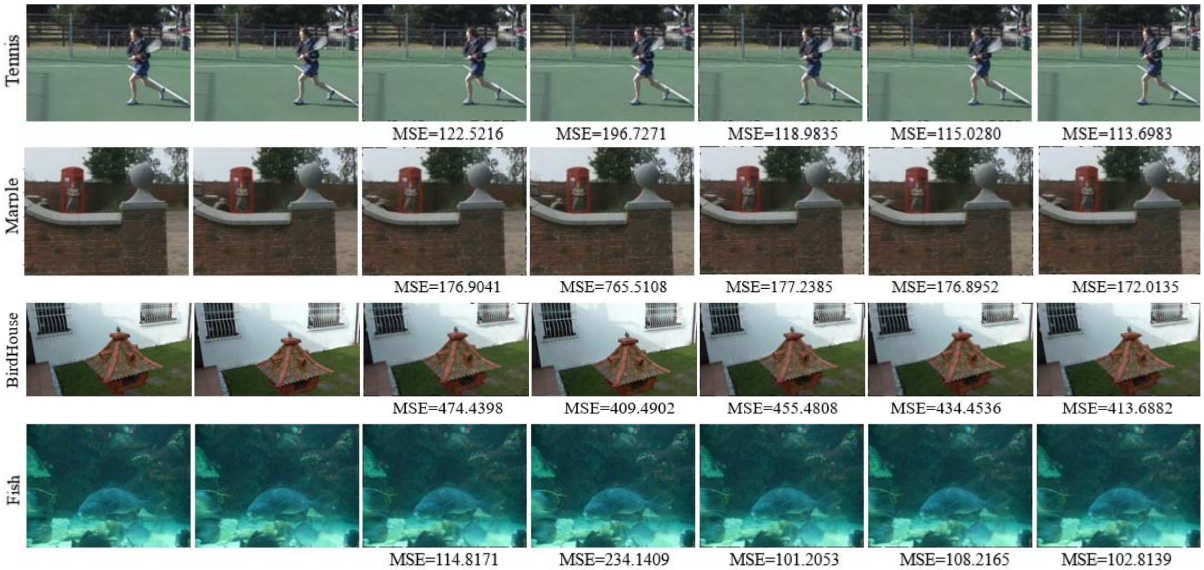

Fig. 13. Experiments on real scene images. The first image of each row is a fixed image and the second image is a moving one, followed by the registration results of Log-Demons, LDDMM, Spectral Log-Demons, Log-Demons with driving force and TDLog-Demons. MSE is below images.

TABLE II
EXPERIMENTS ON BRAIN IMAGE REGISTRATION

Dice coefficient	Log-Demons	LDDMM	Spectral Log-Demons	Log-Demons with driving force	TDLog-Demons
WM	0.4481($\pm$0.0656)	0.4288($\pm$0.0778)	0.4484($\pm$0.0662)	0.4484($\pm$0.0675)	0.4483($\pm$0.0648)
GM	0.7875($\pm$0.0153)	0.7203($\pm$0.0170)	0.7874($\pm$0.0159)	0.7878($\pm$0.0184)	0.7879($\pm$0.0157)
CSF	0.8944($\pm$0.0242)	0.8176($\pm$0.0286)	0.8945($\pm$0.0235)	0.8947($\pm$0.0286)	0.8948($\pm$0.0234)
MSE	461.71($\pm$91.56)	884.76($\pm$98.67)	462.77($\pm$90.29)	459.16($\pm$97.56)	457.19($\pm$97.06)

Table II shows the MSE and dice coefficient of the five methods. It can be seen that LDDMM is the worst and TDLog-Demons outperforms Log-Demons, Spectral Log-Demons and Log-Demons with a driving force in GM and CSF. The experimental results detailed in Supplementary File show that it performs well for brain image segmentation.

The above experiments conclude that the performance of TDLog-Demons is superior to other Log-Demons methods on real images, and the structural tensor and the driving force integrated into Log-Demons can lead to a more precise result.

V. CONCLUSION

In this paper, we propose a structural tensor and driving force-based Log-Demons algorithm for large-deformation image registration. We propose to use a driving force to deal with large deformation and a structure tensor to obtain a smooth and accurate deformation field. When the deformation is large, the driving force plays an important role. When it is small, the structural tensor, which acquires image details, enables Log-Demons to obtain a smoother deformation. Thus the proposed TDLog-Demons not only captures large deformations but also preserves image details, thereby achieving the best accuracy in comparison with three state-of-the-art methods. Experimental results fully demonstrate the conclusion.

ACKNOWLEDGMENT

The authors would like to thank Herve Lombaert, Laurent Risser, and Bin Fan for sharing their code.

REFERENCES

[1] Y. Zeng, C. Wang, X. Gu, D. Samaras, and N. Paragios, "Higher-order graph principles towards non-rigid surface registration," *IEEE Trans. Pattern Anal. Mach. Intell.*, vol. 38, no. 12, pp. 2416–2429, Dec. 2016.

[2] R. Shenoy, M.-C. Shih, and K. Rose, "Deformable registration of biomedical images using 2D hidden Markov models," *IEEE Trans. Image Process.*, vol. 25, no. 10, pp. 4631–4640, Oct. 2016.

[3] W. Shao *et al.*, "Population shape collapse in large deformation registration of MR brain images," in *Proc. IEEE Conf. Comput. Vis. Pattern Recognit.*, Jun./Jul. 2016, pp. 549–557.

[4] W. Wang and X. Yuan, "Recent advances in image dehazing," *IEEE/CAA J. Autom. Sinica*, vol. 4, no. 3, pp. 410–436, Jan. 2017.

[5] M. Tan and A. Qiu, "Large deformation multiresolution diffeomorphic metric mapping for multiresolution cortical surfaces: A coarse-to-fine approach," *IEEE Trans. Image Process.*, vol. 25, no. 9, pp. 4061–4074, Sep. 2016.

[6] L. Geng, Z. Ji, Y. Yuan, and Y. Yin, "Fractional-order sparse representation for image denoising," *IEEE/CAA J. Autom. Sinica*, vol. 5, no. 2, pp. 555–563, Mar. 2018.

[7] L. Bao, Q. Yang, and H. Jin, "Fast edge-preserving PatchMatch for large displacement optical flow," *IEEE Trans. Image Process.*, vol. 23, no. 12, pp. 4996–5006, Dec. 2014.

[8] J.-P. Thirion, "Image matching as a diffusion process: An analogy with Maxwell's demons," *Med. Image Anal.*, vol. 2, no. 3, pp. 243–260, 1998.

[9] X. Pennec, P. Cachier, and N. Ayache, "Understanding the 'demon's algorithm': 3D non-rigid registration by gradient descent," in *Medical Image Computing and Computer-Assisted Intervention—MICCAI*. Berlin, Germany: Springer, 1999, pp. 597–605.

[10] P. Cachier, E. Bardinet, D. Dormont, X. Pennec, and N. Ayache, "Iconic feature based nonrigid registration: The PASHA algorithm," *Comput. Vis. Image Understand.*, vol. 89, nos. 2–3, pp. 272–298, 2003.

[11] B. Biswas, A. Chakrabarti, and K. N. Dey, "Image registration method using Harris Corner and modified Hausdorff distance with near set," in *Proc. IEEE Int. Conf. Recent Trends Inf. Syst.*, Jul. 2015, pp. 393–398.

[12] T. Mansi, X. Pennec, M. Sermesant, H. Delingette, and N. Ayache, "iLogDemons: A demons-based registration algorithm for tracking incompressible elastic biological tissues," *Int. J. Comput. Vis.*, vol. 92, no. 1, pp. 92–111, 2011.

[13] D. Rueckert, P. Aljabar, R. A. Heckemann, J. V. Hajnal, and A. Hammers, "Diffeomorphic registration using B-splines," in *Proc. 9th Int. Conf. Med. Image Comput. Comput.-Assist. Intervent. (MICCAI)*, 2006, pp. 702–709.

[14] M. F. Beg, M. I. Miller, A. Trouvé, and L. Younes, "Computing large deformation metric mappings via geodesic flows of diffeomorphisms," *Int. J. Comput. Vis.*, vol. 61, no. 2, pp. 139–157, 2005.

[15] X. Yang, Y. Li, D. Reutens, and T. Jiang, "Diffeomorphic metric landmark mapping using stationary velocity field parameterization," *Int. J. Comput. Vis.*, vol. 115, no. 2, pp. 69–86, 2015.

[16] H. Wang *et al.*, "Validation of an accelerated 'demons' algorithm for deformable image registration in radiation therapy," *Phys. Med. Biol.*, vol. 50, no. 12, pp. 2887–2906, 2005.

[17] T. Brox and J. Malik, "Large displacement optical flow: Descriptor matching in variational motion estimation," *IEEE Trans. Pattern Anal. Mach. Intell.*, vol. 33, no. 3, pp. 500–513, Mar. 2011.

[18] C. Liu, J. Yuen, A. Torralba, J. Sivic, and W. T. Freeman, "SIFT flow: Dense correspondence across different scenes," in *Proc. Eur. Conf. Comput. Vis.*, 2008, pp. 28–42.

[19] S. Benhimane and E. Malis, "Real-time image-based tracking of planes using efficient second-order minimization," in *Proc. IEEE Int. Conf. Intell. Robots Syst.*, vol. 1, Sep. 2004, pp. 943–948.

[20] T. Vercauteren, X. Pennec, A. Perchant, and N. Ayache, "Diffeomorphic demons: Efficient non-parametric image registration," *NeuroImage*, vol. 45, pp. S61–S72, Mar. 2009.

[21] T. Vercauteren, X. Pennec, A. Perchant, and N. Ayache, "Symmetric log-domain diffeomorphic registration: A demons-based approach," in *Proc. MICCAI*, 2008, pp. 754–761.

[22] T. Vercauteren, X. Pennec, E. Malis, A. Perchant, and N. Ayache, "Insight into efficient image registration techniques and the demons algorithm," in *Proc. 20th Biennial Int. Conf. Inf. Process. Med. Imag.*, Kerkrade, The Netherlands, Jul. 2007 pp. 495–506.

[23] D. G. Lowe, "Distinctive image features from scale-invariant keypoints," *Int. J. Comput. Vis.*, vol. 60, no. 2, pp. 91–110, 2004.

[24] E. Tola, V. Lepetit, and P. Fua, "A fast local descriptor for dense matching," in *Proc. IEEE Conf. Comput. Vis. Pattern Recognit.*, Jun. 2008, pp. 1–8.

[25] B. Fan, F. Wu, and Z. Hu, "Rotationally invariant descriptors using intensity order pooling," *IEEE Trans. Pattern Anal. Mach. Intell.*, vol. 34, no. 10, pp. 2031–2045, Oct. 2012.

[26] N. Dalal and B. Triggs, "Histograms of oriented gradients for human detection," in *Proc. IEEE Comput. Soc. Conf. Comput. Vis. Pattern Recognit.*, vol. 1, Jun. 2005, pp. 886–893.

[27] A. Cifor, L. Risser, D. Chung, E. M. Anderson, and J. A. Schnabel, "Hybrid feature-based log-demons registration for tumour tracking in 2-D liver ultrasound images," in *Proc. IEEE Int. Symp. Biomed. Imag.*, May 2012, pp. 724–727.

[28] H. Lombaert, L. Grady, X. Pennec, N. Ayache, and F. Cheriet, "Spectral demons—Image registration via global spectral correspondence," in *Proc. Eur. Conf. Comput. Vis.*, Firenze, Italy, Oct. 2012, pp. 30–44.

[29] H. Lombaert, L. Grady, X. Pennec, N. Ayache, and F. Cheriet, "Spectral log-demons: Diffeomorphic image registration with very large deformations," *Int. J. Comput. Vis.*, vol. 107, no. 3, pp. 254–271, 2014.

[30] K. Lin, N. Jiang, S. Liu, L.-F. Cheong, M. Do, and J. Lu, "Direct photometric alignment by mesh deformation," in *Proc. IEEE Conf. Comput. Vis. Pattern Recognit.*, Jul. 2017, pp. 2701–2709.

[31] C. Seiler, X. Pennec, and M. Reyes, "Geometry-aware multiscale image registration via OBBTree-based polyaffine log-demons," in *Proc. 14th Int. Conf. Med. Image Comput. Comput.-Assist. Intervent.*, Toronto, ON, Canada, Sep. 2011. pp. 631–638.

[32] V. Siless *et al.*, "Joint T1 and brain fiber log-demons registration using currents to model geometry," in *Proc. 15th Int. Conf. Med. Image Comput. Comput.-Assist. Intervent.*, Nice, France, Oct. 2012, pp. 57–65.

[33] *Simulated Brain Database*. [Online]. Available: http://www.bic.mni.mcgill.ca/brainweb/

[34] H. H. Chang, A. H. Zhuang, D. J. Valentino, and W. C. Chu, "Performance measure characterization for evaluating neuroimage segmentation algorithms," *NeuroImage*, vol. 47, no. 1, pp. 122–135, 2009.

[35] *Human-Assisted Motion Annotation*. Accessed: 2008. [Online]. Available: http://people.csail.mit.edu/celiu/motionAnnotation

[36] M. Jenkinson, C. F. Beckmann, T. E. Behrens, M. W. Woolrich, and S. M. Smith, "FSL," *NeuroImage*, vol. 62, no. 2, pp. 782–790, 2012.

[37] S. Di Zenzo, "A note on the gradient of a multi-image," *Comput. Vis., Graph., Image Process.*, vol. 33, no. 1, pp. 116–125, 1986.

[38] J. Weickert, *Anisotropic Diffusion In Image Processing*, vol. 16. Stuttgart, Germany: B.G. Teubner, 1998, p. 272.

[39] L. Zhang and Y. Wen, "Log-demons with driving force for large deformation image registration," in *Proc. Int. Joint Conf. Neural Netw.*, 2016, pp. 3052–3059.

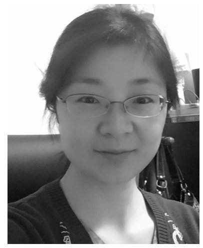

Ying Wen received the B.S. degree in industrial automation from the Technology of Hefei University, China, in 1997, the M.S. degree in imaging processing and pattern recognition from Shanghai University, China, in 2002, and the Ph.D. degree in imaging processing and pattern recognition from Shanghai Jiao Tong University, in 2009. From 2002 to 2009, she was a Senior Engineer with the Ministry of Posts and Telecommunications. She was a Post-Doctoral Research Fellow at the Pediatric Brain Imaging Laboratory, Columbia University, New York, NY, USA, from 2009 to 2011. She currently is a Professor with the East China Normal University. Her research interests include image processing, pattern recognition, machine learning, and computer vision.

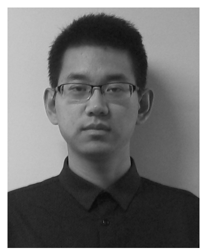

Le Zhang received the B.E. degree in computer science and technology from the Institute of Technology, Shanghai, China, in 2013. He is currently pursuing the master's degree in pattern recognition and intelligent systems with the East China Normal University, Shanghai. His research interests include pattern recognition and image processing.

LiangHua He received the B.S. degree in surveying and mapping from the Wuhan Technology University of Surveying and Mapping, Wuhan, China, in 1999, the M.S. degree in surveying and mapping from Wuhan University, Wuhan, in 2002, and the Ph.D. degree in electronic engineering from Southeast University, Nanjing, China, in 2005. From 2005 to 2007, he was with Tongji University, Shanghai, China, as a Post-Doctoral Researcher. Since 2007, he has been with the Department of Computer Science and Technology, Tongji University, where he is currently a Professor. His research interests include cognition computing, image understanding, and machine learning.

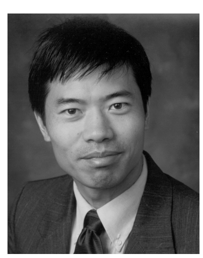

MengChu Zhou (S'88–M'90–SM'93–F'03) received the B.S. degree in control engineering from the Nanjing University of Science and Technology, Nanjing, China, in 1983, the M.S. degree in automatic control from the Beijing Institute of Technology, Beijing, China, in 1986, and the Ph.D. degree in computer and systems engineering from the Rensselaer Polytechnic Institute, Troy, NY, USA, in 1990. He joined the New Jersey Institute of Technology (NJIT), Newark, NJ, USA, in 1990, where he is currently a Distinguished Professor of electrical and computer engineering. His research interests are in Petri nets, intelligent automation, the Internet of Things, big data, web services, and intelligent transportation. He has over 800 publications, including 12 books, over 500 journal papers (more than 380 in IEEE transactions), 12 patents, and 29 book chapters. He is a fellow of the International Federation of Automatic Control (IFAC) and the American Association for the Advancement of Science (AAAS). He was a recipient of the Humboldt Research Award for U.S. Senior Scientists from the Alexander von Humboldt Foundation, the Franklin V. Taylor Memorial Award, and the Norbert Wiener Award from IEEE Systems, Man and Cybernetics Society. He is the Founding Editor of the IEEE Press Book Series on Systems Science and Engineering. He is a Life Member of the Chinese Association for Science and Technology-USA and served as its President in 1999.